Plasma-wall boundary layers

V. Baritello, F. Porcelli, and F. Subba
Istituto Nazionale di Fisica della Materia and Politecnico di Torino, 10129 Torino, Italy
(Received 4 November 1998; revised manuscript received 10 May 1999)

According to a well established result, boundary layers develop in plasmas near solid surfaces. By means of a one-dimensional two-fluid model, we analyze the influence of charge separation and ion viscosity upon the layer structure. This leads to a critical discussion of the Bohm criterion. We find that, in the viscous limit, quasineutrality holds even at values of the Mach number above unity. A nonlinear boundary value problem is defined. Asymptotic matching techniques are used to resolve the structures of the boundary layers. [S1063-651X(99)12709-0]

PACS number(s): 52.40.−w

I. INTRODUCTION

The insertion of a solid surface into a plasma leads to the formation of a boundary layer [1–3], i.e., a region characterized by a strong variation of the principal plasma properties. In the present paper we shall identify this layer with the region of suprathermal ion fluid velocity. This problem is relevant to plasmas of thermonuclear as well as industrial interest. In a fusion plasma, fuel ions (normally deuterium and tritium nuclei) hitting the wall cause the release of heavy ion impurities (sputtering), contaminating the plasma and enhancing radiative thermal losses. As for plasma of industrial interest, the wall bombardment is exploited for the deposition of thin films and the formation of microstructures on the surface of semiconductors (plasma etching).

Our investigation employs a two-fluid plasma model. However, fluid theory is not complete, and it is clear that a consistent theory of the sheath should employ the kinetic approach [4,5]. In particular, the value of the electrostatic potential at the wall (the so-called *floating potential*) is determined by kinetic considerations [6]. If the wall is biased, the wall potential relative to the plasma can be controlled externally. The fluid approach is very promising in modeling some of the main features of the sheath physics, because it allows one to employ much simpler mathematical tools [7]. A possible compromise, adopted in this paper, is to utilize the value of the wall potential as a free parameter; in the case of unbiased walls, this value must correspond to that determined by kinetic theory. However, this approach gives rise to some inconsistencies, especially in the case where ion viscosity is important, which will be pointed out later in the paper.

A relevant criterion which characterizes the presence of a boundary layer is the so called Bohm criterion [8]. This states that a small electric field extends into the plasma and is sufficient to accelerate the ions such that at the entrance of the layer they attain a drift velocity equal to the thermal speed [6,3,9,10]. A widespread opinion is that quasineutrality breaks down in the layer, where the ion velocity exceeds the thermal speed. In this paper, we show that ion viscosity can allow quasineutrality to be kept even at values of the Mach number [11] exceeding unity. We also discuss how the ionic source changes as a function of the wall potential in such a way that, under stationary conditions, it becomes the eigenvalue of the mathematical model.

The layout of the paper is as follows. In Sec. II we present the fluid model equations, and we state a minimal set of boundary conditions. In the plasma region outside the layer, a simplified *ideal* model can be used, where quasineutrality is assumed and dissipation can be neglected. In Sec. III we point out the appearance of a singularity corresponding to the Mach surface $M=1$. We also discuss two types of sources: $S=\text{const}$ and $S\propto n$, where n is the charged particle density. In Sec. IV we consider the boundary layer structure [12] in the nonviscous limit. We also discuss the special role of the normalized ion source S as the eigenvalue of the model. In Sec. V, we consider the effects of a finite ion viscosity on the boundary layer structure. In both Secs. IV and V we compare the complete numerical solutions with those obtained by means of asymptotic matching techniques [12]. In Sec. VI, we discuss our results.

II. FLUID MODEL

We study a stationary model for a fully ionized plasma composed by electrons and one singly charged ion species starting from Braginskii equations [13]. The simplest geometry is a one-dimensional box $-L\leqslant z\leqslant L$, limited by two walls at $z=\pm L$. Moreover, for the sake of simplicity, we consider the magnetic field to be absent or aligned along the z direction, which is normal to the walls, so that it will not appear explicitly in the model equations. For realistic situations, in controlled fusion experiments, the field lines may intersect the wall with a small angle, and thus the ions can be scraped off from a stand-off distance of a Larmor radius, creating a presheath [10,14]. We do not treat this case here. Nevertheless, we point out that recent investigations of resistive interchange instabilities on open field lines relevant to tokamak scrape-off layers adopt the same geometry as in this paper as far as magnetic field lines are concerned [15]. Assuming that the electrons follow the Boltzmann law, which is reasonable due to their high mobility, then, neglecting terms of order $m_e/m_i\ll 1$, the ion dynamics decouples from that of the electrons. Another simplification we adopt is that of constant temperatures. Mass and momentum balance, together with Poisson's and Boltzmann's laws, yield the fluid model for the variables n_i, v_i, φ, and n_e,

$$\frac{d}{dz}(n_i v_i) = S_i, \tag{1}$$

$$m_i n_i v_i \frac{dv_i}{dz} = -T_i \frac{dn_i}{dz} - e n_i \frac{d\varphi}{dz} + \frac{d}{dz}\left(\mu \frac{dv_i}{dz}\right) - m_i S_i v_i, \tag{2}$$

$$n_e = n_0 \exp\left(\frac{e\varphi}{T_e}\right), \tag{3}$$

$$\frac{d^2\varphi}{dz^2} = 4\pi e(n_e - n_i). \tag{4}$$

In these equations, $n_{i(e)}$ is the ion (electron) density, v_i is the ion fluid velocity, S_i is the ion source, $m_{i(e)}$ is the ion (electron) mass, $-e$ is the electron charge, φ is the electrostatic potential, $T_{i(e)}$ is the ion (electron) temperature, and $\mu \simeq n_i \lambda_i (m_i T_i)^{1/2}$ is the ion viscosity coefficient, with λ_i the collisional mean free path [13]. Note that $\lambda_i \propto T_i^2/n_i$, so that for $T_i = \text{const}$ the coefficient μ does not depend on z. We consider a singly charged ion species (the charge is $+e$).

Under the assumption of stationary equilibrium, the electron and ion currents, $J_{e,i} = \mp e n_{e,i} v_{e,i}$, must be equal at the wall. The model assumes that one electron and one positive ion neutralize at the wall and then recycle as a neutral atom, which ionizes at some distance from the wall into the plasma, giving rise to the ionization source profile $S_i(x)$ in Eq. (1). The situation we describe corresponds to full charge recycling.

We now introduce the dimensionless quantities

$$x = \frac{z}{L}, \quad \zeta = \frac{e\varphi}{T_e}, \quad S = \frac{L S_i}{n_0 c_s}, \tag{5}$$

$$M = \frac{v_i}{c_s}, \quad \varepsilon = \frac{\lambda_D}{L}, \quad n = \frac{n_i}{n_0}, \quad \gamma = \frac{\mu}{m_i n_0 c_s L} \equiv \frac{1}{R_e}, \tag{6}$$

where $c_s = \sqrt{(T_e + T_i)/m_i}$ is the thermal speed, L is the half width of our domain, n_0 is the ion density at the midplane location $(z=0)T$, $\lambda_D = (T_e/4\pi n_0 e^2)^{1/2}$ is the Debye length, $M = v_i/c_s$ is the Mach number, and R_e is the Reynolds' number. Expressing μ in terms of the ion temperature, density, and mass, we can also write $\gamma \sim [T_i/(T_i+T_e)]^{1/2} \lambda_i / L$. With these normalizations, Eqs. (1)–(4) become

$$\frac{d}{dx}(nM) = S, \tag{7}$$

$$nM \frac{dM}{dx} = -n \frac{d\zeta}{dx} - \alpha^2 \left(\frac{dn}{dx} - n \frac{d\zeta}{dx}\right) + \gamma \frac{d^2 M}{dx^2} - SM, \tag{8}$$

$$\varepsilon^2 \frac{d^2\zeta}{dx^2} = \exp(\zeta) - n, \tag{9}$$

where $\alpha = [T_i/(T_i+T_e)]^{1/2}$, and we have used Boltzmann's law [Eq. (3)] to eliminate n_e.

A complete set of boundary conditions for the model is

$$\zeta(0) = 0, \ \ \zeta'(0) = 0, \ \ \zeta(\pm 1) = \zeta_{\text{wall}}. \tag{10}$$

The corresponding conditions on n and M can be obtained from those for the normalized electrostatic potential ζ. In particular, the first condition is a reference value for the potential, while the second is suggested by symmetry considerations. The last boundary condition introduces the parameter ζ_{wall}, which from kinetic considerations equals the floating potential $\zeta_{\text{wall}} = \zeta_{\text{float}}$, where

$$\zeta_{\text{float}} = \ln(m_e T_i / m_i T_e)^{1/2}. \tag{11}$$

Note that the choice $\zeta(1) = \zeta(-1)$, together with S, an even function of z, introduces a parity for the relevant solutions such that $n(z) = n(-z)$, $\zeta(z) = \zeta(-z)$ and $M(z) = M(-z)$.

III. IDEAL REGION

Equations (7)–(9) form a strongly nonlinear system which, together with Eq. (10), involves the formation of boundary layers. The parameters ε and γ appearing in these equations are typically very small. Therefore, the terms they multiply will be important only in a narrow region near the wall, where the velocity and the potential vary rapidly. Far from the walls, in the ideal region, these terms can be neglected. In the limit $\varepsilon, \gamma \to 0$, Eqs. (7)–(9) can be rewritten in the forms

$$\frac{d}{dx}(nM) = S, \tag{12}$$

$$nM \frac{dM}{dx} = -n \frac{d\zeta}{dx} - SM, \tag{13}$$

$$\exp(\zeta) - n = 0. \tag{14}$$

Note that the term depending on α disappears in the ideal region because of the quasineutrality assumption. From Eqs. (12) and (13), we can write the following relation for the ion velocity:

$$(1 - M^2) \frac{dM}{dx} = \frac{S}{n}(1 + M^2). \tag{15}$$

Equation (15) clearly shows the appearance of a singularity in the ideal solution corresponding to Mach number $M = 1$. It is interesting to express this singularity condition in terms of the potential ζ. To this aim we consider the density n as a function of the ion velocity: $n = n(M)$. If we use the continuity equation (12) to eliminate the source S in Eq. (13), we obtain an equation for dn/dM, whose solution is [6]

$$n = \frac{1}{1 + M^2}, \tag{16}$$

from which we obtain

$$\zeta = -\ln(1 + M^2). \tag{17}$$

In particular, Eq. (17) states that the singularity of the ideal solution corresponds to the potential value $\zeta = -\ln(2)$. The electric field $E = -d\zeta/dx$ diverges at this point. Generally, from Eqs. (12) and (16) it is possible to write the expression

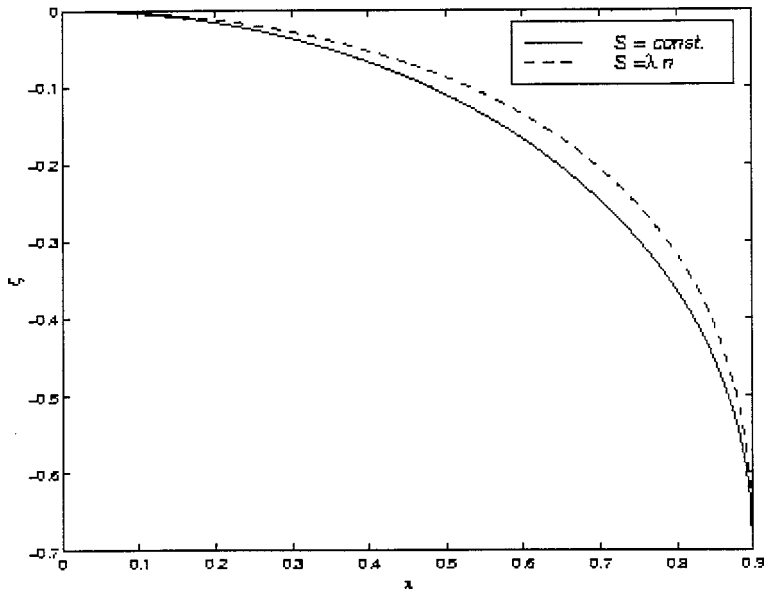

FIG. 1. Potential profiles in the ideal region for two different types of sources. Line (1) refers to the choice $S=\text{const}$, while line (2) corresponds to $S=\lambda n$. The two curves are matched so as to have a singularity at $x=0.9$. Correspondingly, we obtain $S=0.556$ for curve (1) and $\lambda=0.634$ for curve (2). (All the plotted quantities are dimensionless).

$$e^{\zeta}\sqrt{e^{-\zeta}-1}=\int_0^x S(x')dx'\equiv G(x). \tag{18}$$

Equation (18) is a biquadratic equation for e^{ζ}. The regular solution in the origin is

$$\zeta(x)=\ln\frac{1}{2}[1+\sqrt{1-4G^2(x)}]. \tag{19}$$

Combining Eq. (16) with Eqs. (17) and (19) gives the corresponding expressions for the density and the ion velocity:

$$n(x)=\frac{1+\sqrt{1-4G^2(x)}}{2}, \tag{20}$$

$$M(x)=\frac{1-\sqrt{1-4G^2(x)}}{2G(x)}. \tag{21}$$

These results are subject to the restriction $0\leqslant G(x)\leqslant 1/2$. If this restriction is satisfied for all the interval $x\in[0,1]$, then no boundary layer develops. However, in this case the wall potential must be $0\geqslant\zeta_{\text{wall}}\geqslant\ln(1/2)$. For more negative values of ζ_{wall}, $G(x)$ must reach the value 1/2 at some distance from the wall. Thus a link between ζ_{wall} and the ion source is established.

Note that no particular hypothesis about the ion source S has been made up to now. A particularly simple choice is $S=\text{const}$. Then, the value of S is determined as an eigenvalue condition in terms of the wall potential. This will be investigated in the next sections. Here we discuss another form for S of interest in many practical situations, where S is determined by the collisions of the electrons with the recycling neutrals [9]. In this case, we may assume the ion source to be proportional to the electron density:

$$S=\lambda\exp(\zeta), \tag{22}$$

where λ is a proportionality constant. Eliminating the source term using Eq. (22) and solving the resulting equation, we obtain

$$M(x)=\tan\{\tfrac{1}{2}[\lambda x+M(x)]\}, \tag{23}$$

from which we obtain

$$\frac{dM}{dx}=\frac{\lambda}{\cos(\lambda x+M)}. \tag{24}$$

As we can see, the singularity is located at the point x_s, which satisfies the relation $\lambda x_s+1=\pi/2$. We may now combine Eqs. (16) and (23) to obtain an expression for the density n. Then Eq. (23) leads to the following implicit relation for the potential:

$$\zeta(x)=2\ln\left(\cos\left\{\frac{1}{2}[\lambda x+\sqrt{\exp(-\zeta(x))-1}]\right\}\right). \tag{25}$$

It is interesting to compare the profile of $\zeta(x)$ obtained by solving Eq. (25) numerically with that in Eq. (19) for the much simpler choice $S=\text{const}$. Figure 1 shows this comparison. The parameters for the two curves are $S=0.556$ and $\lambda=0.634$, which give the same value of $x_s=0.9$ in the two cases. As we can see immediately, the profiles are very close to each other. For this reason, in the following we shall refer to the simplest choice $S=\text{const}$, except if stated otherwise.

IV. NONDISSIPATIVE BOUNDARY LAYER

In principle, the complete (i.e., up to the wall) potential profile in the non dissipative limit may be obtained by solving a single third-order differential equation. To show this, we introduce the new independent variable $y=x^2$ and the function

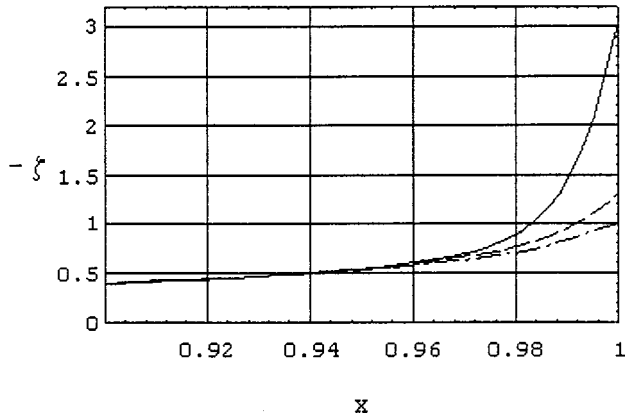

FIG. 2. Potential profiles numerically calculated for different values of the Debye length: rotating clockwise, we obtain $\varepsilon=3\times10^{-3}$, $\varepsilon=5\times10^{-3}$ and $\varepsilon=7\times10^{-3}$, respectively. For all cases, $S=0.52$. (All the plotted quantities are dimensionless.)

$$w(y)=-\int_0^y \zeta(\sqrt{y'})\,dy'. \tag{26}$$

Then, from Eqs. (7)–(9), with $S=\text{const}$, we obtain

$$\varepsilon^2[4yw'''(y)+2w''(y)]-\frac{Sy}{[2(yw'(y)-w(y))]^{1/2}} +\exp[-w'(y)]=0. \tag{27}$$

The corresponding boundary conditions are

$$w(0)=0,\quad w'(0)=0,\quad w'(1)=-\zeta_{\text{wall}}. \tag{28}$$

Conditions (28) are immediately evident from the definition of w and conditions (10) for ζ. It is not difficult to give a physical interpretation of S as an eigenvalue for the boundary value problems (27) and (28). Particle conservation implies $S_i z_s=n_s c_s$, which can be rewritten as $S=Ln_s/z_s n_0$ where $n_s=n(z_s)$ and z_s is the location where $M(z_s)=1$ for the complete solution. It is now intuitive that $Ln_s/z_s n_0$ depends on ζ_{wall}. Also note that since $n_s\sim0.5n_0$, the value of S will stay approximately close to one-half. In Figs. 2 and 3, we

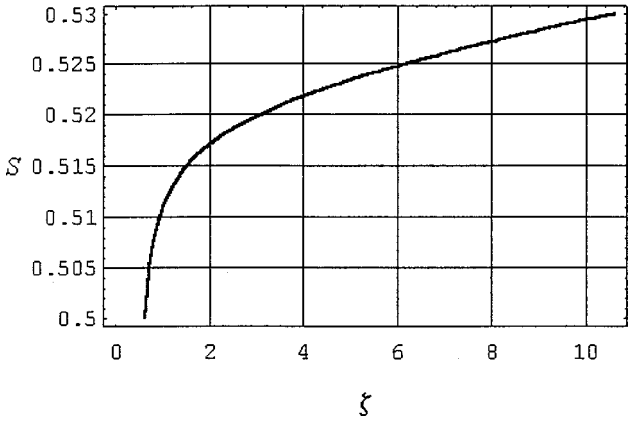

FIG. 3. Dependence of the source eigenvalue S on the wall potential ζ_{wall}. The normalized Debye length is $\varepsilon=3\times10^{-3}$. (All the plotted quantities are dimensionless.)

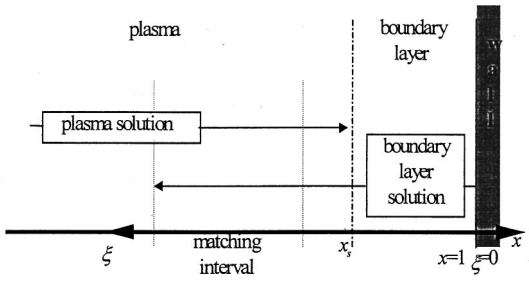

FIG. 4. Schematic view of the geometry of the matching interval between the plasma and the sheath potential profiles. (All the plotted quantities are dimensionless.)

show numerical solutions for the electrostatic potential for different values of ϵ and the dependence of the source eigenvalue on the wall potential.

It is natural to try and find an approximate solution of Eq. (27) by asymptotic matching techniques. First of all, we try to estimate the boundary layer thickness. As discussed in Sec. III, a boundary layer forms for $S>\frac{1}{2}$. As it appears from Eqs. (18) and (19), the singular point x_s for the ideal solution is a function of the normalized source S. For $S=\text{const}$, we obtain $x_s=1/2S$. Then, the boundary layer thickness may be estimated as $\Delta=1-1/2S$. For typical plasma parameters, numerical calculations show that $\Delta\leqslant10^{-2}$ in correspondence to $\epsilon\simeq10^{-6}$ and $\zeta_{\text{wall}}\simeq\zeta_{\text{floating}}$. In order to find an equation for the potential near the solid wall, we introduce the layer variable $\xi=(x-x_s)/\epsilon$. Referring to Fig. 4, we see that the *outer* or ideal solution holds up to x_s (i.e., the beginning of the layer). In particular, the electrostatic potential in the layer (inner region) should obey a simplified differential equation with boundary condition $\zeta=\zeta_{\text{wall}}$ at $\xi=(1-x_s)/\epsilon$. An overlapping region [12] where the ideal equation holds and the layer equation is valid must exist for the matching to be possible. As can be seen from Fig. 4, this interval lies entirely to the left ($\xi<0$) of the singular point x_s.

The layer equation must be solved subject to the condition that it matches asymptotically to the ideal solution within the overlapping interval. We propose the following layer equation:

$$\frac{1}{2}\left(\frac{d\zeta}{d\xi}\right)^2=e^{\zeta(\xi)}+\left[\frac{1}{2}(D-\zeta(\xi)) -\theta(-\xi)\left(S\varepsilon\xi+\frac{8}{3}(-S\varepsilon\xi)^{3/2}\right)\right]^{1/2} +\theta(-\xi)[S\varepsilon\xi+2(-S\varepsilon\xi)^{3/2}]+C, \tag{29}$$

where $\theta(y)$ is the Heaviside function. This equation is derived in the Appendix. We find it necessary to retain terms of order $\epsilon^{3/2}$, as these terms are essential to reproduce the correct behavior of the layer solution in the matching interval. In particular, the constants C and D are integration constants to be determined by asymptotic matching. Unfortunately, Eq. (29) cannot be solved analytically. Nonetheless, it is much simpler than Eq. (27), which is valid over the entire plasma region. Thus we can solve Eq. (29) by a simple numerical procedure. We point out that, once the suitable matching interval is determined numerically, the integration constants C and D are practically insensitive to the specific point

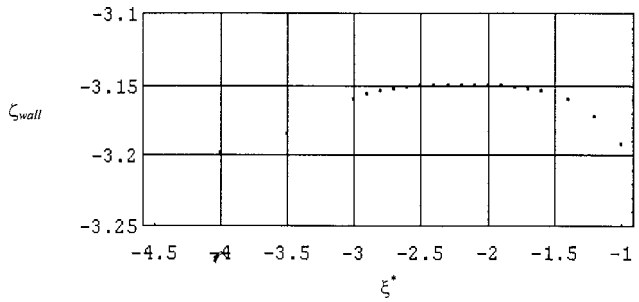

FIG. 5. Dependence of $\zeta_{\rm wall}$ on ξ^*. The constancy of $\zeta_{\rm wall}$ for ξ^* varying in the interval $(-2.5, -2.0)$ clearly shows the matching interval. (All the plotted quantities are dimensionless.)

within that interval where they are evaluated. The integration constants C and D are to be determined in such a way that the boundary layer solution and the ideal solution have the same functional form in the overlapping (matching) region for a given value of $\zeta_{\rm wall}$. Thus we determine these constants by imposing that both the inner and ideal solutions have the same first and second derivatives in a suitable point ξ^* of the overlapping interval.

The numerical determination of the matching interval is illustrated in Fig. 5. One can see that $\zeta_{\rm wall}$ is practically independent of the choice of ξ^* for $\xi_1<\xi^*<\xi_2$ with $\xi_1=-2.5$ and $\xi_2=-2.0$ determined numerically for the chosen parameters $\epsilon=0.003$ and $\zeta_{\rm wall}=-3.15$. In this case, we obtain $S\simeq 0.52$, $C\simeq 0.995$, and $D\simeq 0.20$.

V. VISCOUS BOUNDARY LAYER

We now consider the viscous case. In the present situation, both the terms depending on γ and ϵ could, in principle, generate a boundary layer. In fact, in most situations of practical interest, the collision mean free path λ_i is usually much larger than the Debye length, over which the electrostatic layer develops. Consequently, we will study the problem in the limit $\epsilon/\gamma\to 0$. In the case of a constant source, we may eliminate M and n from Eqs. (7)–(9) and obtain a second order differential equation for the electrostatic potential ζ,

$$\gamma Sx\frac{d^2\zeta}{dx^2}+(2\gamma S-S^2x^2+e^{2\zeta(x)})\frac{d\zeta}{dx}-\gamma Sx\left(\frac{d\zeta}{dx}\right)^2+2S^2x=0, \tag{30}$$

subject to the boundary conditions

$$\zeta(0)=0,\quad \zeta(1)=\zeta_{\rm wall}. \tag{31}$$

Note that the condition $\zeta'(0)=0$ is now implied by Eqs. (30) and (31). Again, this equation defines a boundary value problem for the eigenvalue S.

A numerical integration of Eq. (30) has been performed for $\gamma=10^{-2}$. The resulting profile is shown in Fig. 6. This figure also shows the potential profile obtained from the more realistic source $S=\lambda n$. As we can see, the two profiles are nearly identical, so the simplifying assumption $S=$const is again not so bad.

It is interesting to evaluate the length scale of the viscosity effects. To this aim, we integrate the continuity equation and write $M(x)=Sxe^{-\zeta(x)}$, from which, in the limit $x\to 1$ with $|d\zeta/dx|\gg 1$, we obtain

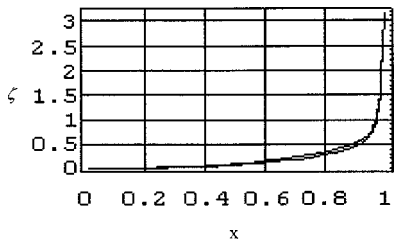

FIG. 6. Potential profiles in the domain $0\leqslant x\leqslant 1$ for $S=$const (dashed line) and $S=\lambda n$ (solid line). The viscosity coefficient is $\gamma=3\times 10^{-3}$ and the source eigenvalues are $S=0.539$ and $\lambda=0.539$, respectively. (All the plotted quantities are dimensionless.)

$$\frac{dM}{dx}\sim Se^{-\zeta(x)}\left(-\frac{d\zeta}{dx}\right)=-Sn\frac{d\zeta}{dx}. \tag{32}$$

Taking account of Eq. (32) and of the relations $\gamma dM/dx\gg 1$ and $nM\sim S$, from Eq. (8) we obtain the dominant balance

$$\gamma\frac{d^2M}{dx^2}\sim S\frac{dM}{dx}. \tag{33}$$

Equation (33) can be integrated to give $M(x)\sim A_1e^{(x-1)S/\gamma}+A_2$, which, as an estimate for the viscous scale length, yields $\delta\sim\gamma/S$. Figure 7 shows a comparison of this estimate with the numerical solution of Eq. (30) for different values of γ/S, where we have defined $\delta\sim[d\ln\zeta(x)/dx]^{-1}_{x=1}$.

Since $S\approx 0.5$, recalling that $\gamma\sim\lambda_i/L$ for $(T_i\sim T_e)$, we find $\delta_\mu\sim\lambda_i$, where δ_μ is the viscous scale length in dimensional units. Thus the validity of this result is marginal with respect to the adopted fluid viscosity operator, which requires the collisional mean free path to be not larger than any other characteristic scale length in the problem. On the other hand, a diffusion-type operator for the transport of plasma momentum may also be justified in terms of fluctuations in a weakly turbulent plasma. The corresponding quantitative estimate for a turbulent viscosity coefficient will be discussed in Sec. VI.

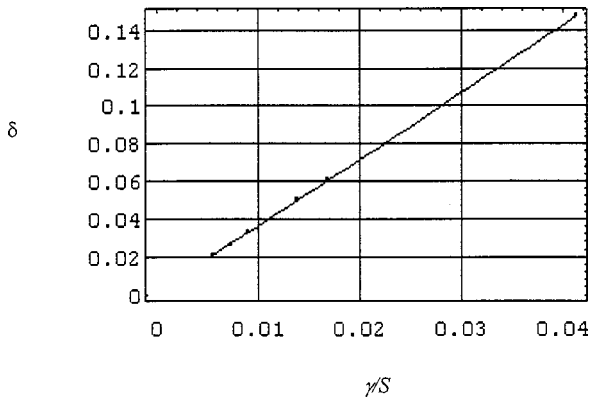

FIG. 7. Width of the viscous layer. The dots represent the value of δ as a function of the ratio γ/s. The eigenvalue S is tuned so as to keep the wall potential fixed at the floating value $\zeta_{\rm wall}\sim -3$, while γ varies in the interval $5\times 10^{-3}\leqslant\gamma\leqslant 3\times 10^{-2}$. The interpolating line outlines the accuracy of the linear scaling of δ as a function of γ/s. (All the plotted quantities are dimensionless.)

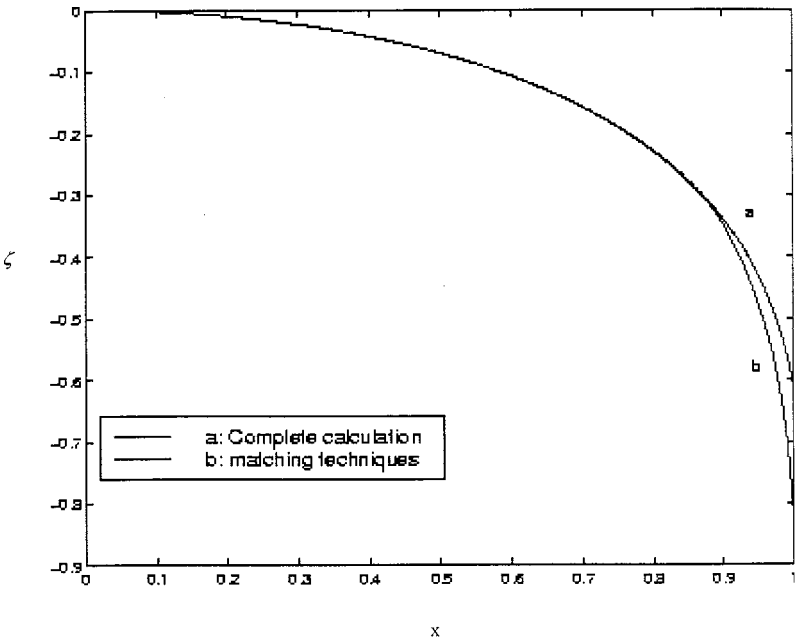

FIG. 8. Comparison of the potential profiles obtained by the numerical solution of the complete equation (a) and by matching techniques (b). For both curves, $S=0.539$ and $\gamma=3\times10^{-3}$. (All the plotted quantities are dimensionless.)

Next we derive a simplified equation for the potential in the boundary layer. In the limit $x\to1$, Eq. (30) becomes

$$\gamma S\frac{d^2\zeta}{dx^2}+(2\gamma S-S^2+e^{2\zeta})\frac{d\zeta}{dx}-\gamma S\left(\frac{d\zeta}{dx}\right)^2+2S^2=0. \tag{34}$$

In the validity domain of the ideal solution, the following relation must be valid:

$$\gamma S\frac{d^2\zeta}{dx^2}\ll 2S^2. \tag{35}$$

Equation (35), combined with the ideal solution (19), is equivalent to

$$1-x/x_s\gg\gamma^{2/3}, \tag{36}$$

with $x_s=1/2S$. Moreover, the ideal solution (19) shows that

$$\frac{d^2\zeta}{dx^2}\gg\left(\frac{d\zeta}{dx}\right)^2,\quad e^{2\zeta(x)}-S^2\gg 2\gamma S. \tag{37}$$

Equations (35) and (37) allow one to write an equation valid in the boundary layer extensible to a matching interval within the ideal region. Introducing the layer variable

$$y=(x-1)S/\gamma, \tag{38}$$

the desired equation takes the form

$$\frac{d^2\zeta}{dy^2}+\left(\frac{1}{S^2}e^{2\zeta(x)}-1\right)\frac{d\zeta}{dy}-\left(\frac{d\zeta}{dy}\right)^2+2\frac{\gamma}{S}=0. \tag{39}$$

Moreover, from Eq. (36) we obtain the following analytic estimate for the matching interval:

$$\gamma^{2/3}\ll 1-\frac{x}{x_s}\ll 1. \tag{40}$$

It is convenient to introduce the new function $u(\zeta)=d\zeta/dy$. With this substitution, Eq. (40) becomes

$$u(\zeta)\frac{du}{d\zeta}+\left(\frac{1}{S^2}\exp(2\zeta)-1\right)u(\zeta)-u^2(\zeta)+2\frac{\gamma}{S}=0. \tag{41}$$

Equation (41) is still too difficult to be solved analytically; however, it can be easily solved numerically. To match correctly the obtained solution with the ideal expression (19), we use the following strategy.

We choose a matching point x_M in the interval defined by Eq. (40); with the aid of Eqs. (19) and (38), we obtain the corresponding values $\zeta_M\equiv\zeta_M(x_M)$, and define $u_M=u(\zeta_M)$. We use u_M as the initial value in the integration of Eq. (41) within the interval $\zeta^*\leqslant\zeta\leqslant\zeta_M$, where ζ^* is chosen smaller than $\zeta_{\rm wall}$. Finally we use $u(\zeta)=d\zeta/dy$ and Eq. (38) to obtain the profile $\zeta(x)$ for the range $x_M\leqslant x\leqslant1$. Figure 8 shows the comparison of the matched solution with the complete one for $\gamma=3\times10^{-3}$ and $S=0.539$. Figure 9 shows how the matching accuracy improves as $\gamma\to0$. We represent the matching accuracy as $|\zeta_{\rm match}(1)-\zeta_{\rm compl}(1)|/\zeta_{\rm compl}(1)$, where $\zeta_{\rm match}(1)=\zeta_{\rm wall}$ obtained for a given S by asymptotic matching while $\zeta_{\rm compl}(1)=\zeta_{\rm wall}$ obtained for the same S by the numerical solution of the complete equation. Figure 10 compares the complete numerical solution and the matching solution for S as a function of $\zeta_{\rm wall}$. The integration of the continuity equation (with $S=$const) yields $nM=Sx$, while quasineutrality gives $n=e^{\zeta}$.

At this point an important question must be raised: what is the appropriate value of $\zeta_{\rm wall}$ to be used in conjunction with the adopted viscous fluid model? If the value $\zeta_{\rm wall}=\zeta_{\rm float}$ is used, as suggested by kinetic theory, for the Mach number at the wall we obtain

$$M_{\rm wall}=Se^{\zeta_{\rm wall}}=(m_iT_e/m_eT_i)^{1/2}S. \tag{42}$$

Assuming a hydrogen plasma with $T_e=T_i$ and $S\simeq\frac{1}{2}$ yields $M_{\rm wall}\simeq20$. This value of $M_{\rm wall}$ is exceedingly large and

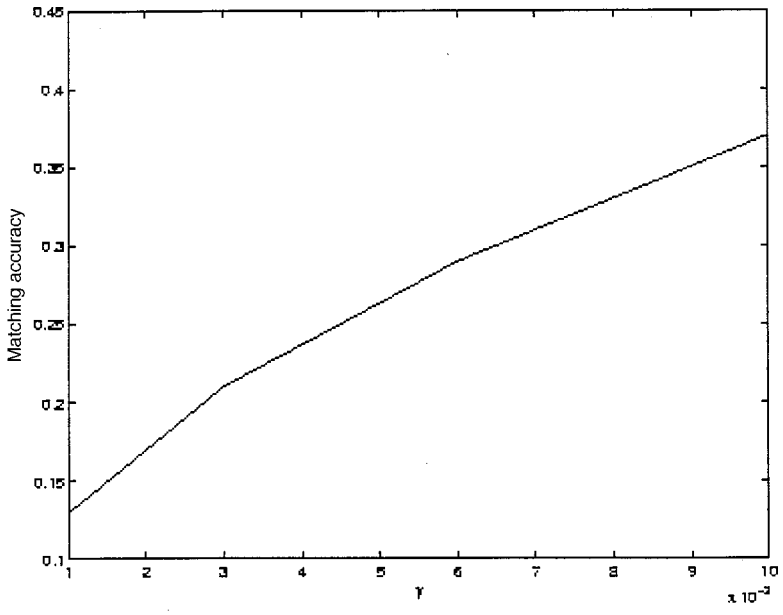

FIG. 9. Matching accuracy $|(\dot{\zeta}_{\mathrm{match}}(1) - \zeta_{\mathrm{comp}}(1))/\zeta_{\mathrm{compl}}(1)|$ as a function of γ. All the calculations are performed with $S=0.502$. (All the plotted quantities are dimensionless.)

clearly violates ion energy conservation; therefore, result (42) must be rejected. It is of interest, however, to understand what goes wrong in this case. As we pointed out in Sec. I, the fluid model is not complete: the concept of floating potential is borrowed from kinetic theory. The point is that the kinetic prescription $\zeta_{\mathrm{wall}}=\zeta_{\mathrm{float}}$ must be used *together* with the kinetic result that the potential drops by a value $O(\zeta_{\mathrm{float}})$ over a distance of the order of the Debye length. Therefore, in the limit where the collisional mean free path is larger than the Debye length, the validity of the fluid model stops a few Debye lengths from the wall, as the model cannot allow spatial variations below λ_i. Thus the boundary value $\zeta=\zeta_{\mathrm{wall}}$ for the fluid equations must be intended as the value of the potential a few Debye lengths from the wall. The appropriate value must be such that M_{wall} remains of order unity, although values $M_{\mathrm{wall}}\geqslant 1$ are allowed. Unfortunately, the present model cannot determine the exact value of ζ_{wall} to be used in the viscous limit.

VI. DISCUSSION AND CONCLUSIONS

In this paper, we have revisited the physics of the boundary layers that form in plasmas near solid surfaces. As a consequence of the high mobility of the electrons relative to that of the ions, the solid surface naturally acquires a negative voltage, as large as a few times T_e/e for the case of floating potential. This negative voltage accelerates the ions to velocities exceeding the thermal speed (Mach numbers $M>1$).

Our investigation has adopted a simplified two-fluid model for the plasma, with the concept of floating potential borrowed from kinetic theory. Clearly, our model is not physically complete; however, it is useful in that it illustrates basic features of the relevant processes and reduces the mathematical treatment to the essential.

From a mathematical point of view, under stationary conditions the model reduces to a nonlinear boundary value problem for the electrostatic potential, with the ion source

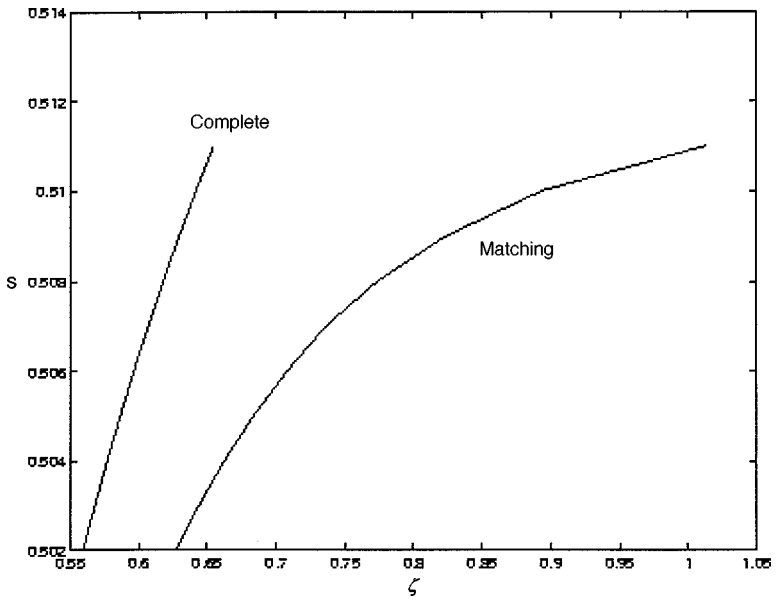

FIG. 10. Source as a function of the wall potential at fixed $\gamma=3\times10^{-3}$. A comparison of the results obtained by integration of the complete equation and by matching techniques is shown. (All the plotted quantities are dimensionless.)

TABLE I. Values of the characteristic parameters of the edge region for different types of plasma. L_c is the connection length, the distance between the solid walls measured along the magnetic field. The other parameters are defined in the text. (All the plotted quantities are dimensionless.)

	JET	DITE	ALCATOR C	Plasma processing
T_e (eV)	50	15	7	1
n_e (cm^{-3})	4×10^{12}	3×10^{12}	4×10^{13}	10^{10}
L_c(cm)	4×10^{3}	4×10^{2}	10^{2}	50
λ_i (cm)	6.4×10^{2}	76	1	13
λ_D (cm)	2.6×10^{-3}	1.7×10^{-3}	3×10^{-4}	7.5×10^{-4}
μ ($\mathrm{g\,cm^{-1}\,s^{-1}}$)	2.8×10^{-2}	1.4×10^{-3}	2.1×10^{-4}	2.1×10^{-6}
ε	6.5×10^{-7}	4.3×10^{-6}	3×10^{-6}	1.5×10^{-5}
γ	1.1×10^{-1}	1.3×10^{-1}	8.5×10^{-3}	1.8×10^{-1}

playing the role of the eigenvalue to be determined as a function of the wall potential. More precisely, we have considered two types of ion sources, $S=\text{const}$ and $S=\lambda n$, with n the normalized ion density and the proportionality constant λ the eigenvalue for this second choice. A useful result is that the obtained solutions are quantitatively very similar in the two cases.

The boundary value problem has been integrated numerically. We have also found approximate solutions by means of asymptotic matching techniques. We have shown that, in order to apply these techniques rigorously, a minimal equation must be considered in the boundary layer. This equation, however, is still nonlinear and too difficult to solve analytically; on the other hand, it is much simpler to solve numerically than the complete boundary layer problem. The strategy to obtain approximate solutions over the entire region by means of this (say semianalytic) approach is illustrated in the paper.

To compare the electrostatic and the viscous limits of the model let us refer to Table I, where values of the relevant parameter for three tokamak fusion experiments [16] [the Joint European Tours (JET), the Divertor Injection Tokamak Experiment (DITE), and the ALCATOR C experiment at the Massachusetts Institute of Technology] and for a typical plasma of industrial interest are considered. We see that, for all these plasmas, the ratio $\epsilon/\gamma\sim\lambda_D/\lambda_i$ is indeed very small, which reflects the fact that the Debye length is normally much smaller than the collisional mean free path.

In the viscous limit, the singularity developed by the ideal equations in correspondence of the region where the Mach number reaches unity is resolved by viscosity. Thus the distance from the wall where M reaches unity is of the order of the ion collisional mean free path, which can be as large as 10% of the connection length (the distance, $2L$, between the two plates in the model; see Table I). This should be of interest, for instance, in the modeling of the edge region of tokamak plasmas, the so called *scrape-off layer*. In fact, the modelling is often based on fluid codes (such as the code EDGE2D adopted at JET [17]) which neglect the boundary layer and assume the boundary condition $M=1$ at the edge of the integration region. This procedure is justified if the boundary layer is very thin; however, this procedure would be questionable if the plasma region where M exceeds unity could become a considerable fraction of the scrape-off layer.

Nevertheless, we point out that results for the viscous limit are marginally valid with respect to the considered viscosity diffusion operator. This operator is derived under the assumption that the collisional mean free path is not larger than any other characteristic length in the plasma, while we have found that the width of the viscous boundary layer is in fact of the order of λ_i. An alternative way of justifying a diffusion operator for the transport of plasma momentum density is by consideration of turbulent transport processes. Suppose that fluctuations introduce a random scattering of the ion trajectories, which can be modeled as a random walk process. Then the turbulent diffusion coefficient becomes $\mu_t\sim m_i n_i \lambda_t^2/\tau_t$, where λ_t and τ_t are, respectively, the characteristic correlation length and correlation time of the fluctuations. Experimental measurements in confined plasmas of thermonuclear interest indicate that transport processes in these plasmas are indeed ''anomalous,'' i.e., they do not follow collisional scaling laws. While theoretical understanding of turbulent transport processes predicting the parameters λ_t and τ_t is still elusive, we can rely on experimental measurements to obtain a quantitative estimate of μ_t. If L_c is the typical size of the plasma (e.g., the connection length) and τ_{expt} is the experimental value of the momentum density confinement time, then we can estimate $\mu_t\sim m_i n_i L_c^2/\tau_{\text{expt}}$. The ''anomalous viscosity'' scale length for the boundary layer by the wall becomes $\delta_t\sim L_c^2/c_s\tau_{\text{expt}}$. Using, for instance, JET parameters with $\tau_{\text{expt}}\sim0.5$ sec, we obtain $\delta_t\sim5$ cm, which is smaller than the collisional mean free path, but still much larger than the Debye length.

ACKNOWLEDGMENTS

This work was supported in part by the National Research Council (CNR) of Italy. Discussions with Drs. A. Taroni and S. Krasheninnikov are gratefully acknowledged.

APPENDIX

In this appendix we present the derivation of Eq. (29). By using the new variable $\xi=(x-x_s)/S$, model equations (7)–(9) take the forms

$$\frac{d}{d\xi}(nM)=\varepsilon S, \tag{A1}$$

$$n(\xi)M(\xi)\frac{dM}{d\xi} = -n\frac{d\zeta}{d\xi} - \varepsilon S M(\xi), \tag{A2}$$

$$\frac{d^2\xi}{d\xi^2} = \exp[\zeta(\xi)] - n(\xi). \tag{A3}$$

The continuity equation (A1) can be easily integrated to give

$$n(\xi)M(\xi) = \tfrac{1}{2} + \varepsilon S\xi, \tag{A4}$$

while Eq. (A2) can be rewritten in the energy conservation form

$$\frac{d}{d\xi}\left(\frac{1}{2}M^2(\xi) + \zeta(\xi)\right) = -\varepsilon S\frac{M(\xi)}{n(\xi)}. \tag{A5}$$

We now look for a suitable form of the Poisson equation. To this aim, we multiply equation (A3) by $d\zeta/d\xi$:

$$\frac{d}{d\xi}\frac{1}{2}\left(\frac{d\zeta}{d\xi}\right)^2 = \frac{d}{d\xi}e^{\zeta(y)} - \frac{1}{2}\frac{1}{M(\xi)}\frac{d\zeta}{d\xi} - \varepsilon\frac{S}{M(\xi)}\xi\frac{d\zeta}{d\xi}. \tag{A6}$$

By dividing (A2) by the product $n(\xi)M(\xi)$, we obtain an expression for the potential derivative:

$$-\frac{1}{M(\xi)}\frac{d\zeta}{d\xi} = \frac{dM}{d\xi} + \varepsilon\frac{S}{n(\xi)}. \tag{A7}$$

We now use Eq. (A7) to eliminate the term $(1/M)d\zeta/d\xi$ in Eq. (A6). The result is

$$\frac{d}{d\xi}\frac{1}{2}\left(\frac{d\zeta}{d\xi}\right)^2 = \frac{d}{d\xi}\left(e^{\zeta(\xi)} + \frac{1}{2}M(\xi)\right) + \frac{1}{2}\varepsilon\frac{S}{n(\xi)} - \varepsilon\frac{S}{M(\xi)}\xi\frac{d\zeta}{d\xi}. \tag{A8}$$

From Eqs. (A5) and (A8), we can derive a model for the boundary layer. In the inner part of the electrostatic sheath, a suitable approximation is obtained simply by neglecting all the terms multiplied by the small parameter ε. It is easy to perform a first integration, and to write

$$\frac{1}{2}\left(\frac{d\zeta}{d\xi}\right)^2 = e^{\zeta(\xi)} + \frac{1}{2}M(\xi) + C, \tag{A9}$$

$$\frac{1}{2}M^2(\xi) + \zeta(\xi) = D, \tag{A10}$$

where C and D are obviously the integration constants. Unfortunately, it turns out that Eqs. (A9) and (A10) do not reproduce the behavior of the ideal solution at the limit of the ideal region; therefore, they cannot be used for asymptotic matching purposes. To obtain a smooth match we must retain terms up to order $\varepsilon^{3/2}$. To this end, we expand the expressions for M and ζ in the ideal region in powers of ε. We obtain the following expressions:

$$M(\xi) \sim \frac{1}{2n(\xi)} \sim 1 - 2(-S\varepsilon\xi)^{1/2}, \tag{A11}$$

$$\frac{1}{2}M^2(\xi)\frac{d\zeta}{d\xi} \sim -(-S\varepsilon\xi)^{1/2}. \tag{A12}$$

If we substitute the last expressions in Eqs. (A5) and (A8), we can obtain two equations corresponding to Eqs. (A9) and (A10):

$$\frac{1}{2}M^2(\xi) + \zeta(\xi) = -2S\varepsilon\xi - \frac{16}{3}(-S\varepsilon\xi)^{3/2} + D, \tag{A13}$$

$$\frac{1}{2}\left(\frac{d\zeta}{d\xi}\right)^2 = e^{\zeta(\xi)} + \frac{1}{2}M(\xi) + S\varepsilon\xi + 2(-S\varepsilon\xi)^{3/2} + C. \tag{A14}$$

Equations (A13) and (A14) allow a good matching with the ideal solution. They are valid in the last part of the ideal region ($\xi \leqslant 0$), while Eqs. (A9) and (A10) refer to the inner part of the boundary layer. We can put the two expressions in a more compact form by introducing the Heaviside function:

$$\theta(y) = \begin{cases} 1, & y > 0 \\ 0, & y < 0 \end{cases}. \tag{A15}$$

Then we write

$$\frac{1}{2}M^2(\xi) + \zeta(\xi) = \theta(-\xi)\left[-2S\varepsilon\xi - \frac{16}{3}(-S\varepsilon\xi)^{3/2}\right] + D, \tag{A16}$$

$$\frac{1}{2}\left(\frac{d\zeta}{d\xi}\right)^2 = e^{\zeta(\xi)} + \frac{1}{2}M(\xi) + \theta(-\xi)[S\varepsilon\xi + 2(-S\varepsilon\xi)^{3/2}] + C. \tag{A17}$$

Finally, eliminating the ion velocity from Eqs. (A16) and (A17), we obtain Eq. (29) in the main text.

[1] L. Tonks and I. Langmuir, Phys. Rev. **34**, 876 (1929).
[2] I. Langmuir, Phys. Rev. **33**, 976 (1929).
[3] P. C. Stangeby, in *Physics of Plasma-Wall Interactions in Controlled Fusion*, edited by D. E. Post and R. Behrisch (Plenum, New York, 1986).
[4] C. A. Ordonez, Phys. Rev. E **55**, 1858 (1997).
[5] S. B. Song, C. S. Chang, and Choi Duk-In, Phys. Rev. E **55**, 1213 (1997).
[6] P. C. Stangeby, Phys. Fluids **27**, 2699 (1984).
[7] M. S. Benilov and G. V. Naidis, Phys. Rev. E **57**, 2230 (1998).
[8] D. Bohm, in *The Characteristics of Electrical Discharges in Magnetic Fields* edited by A. Guthrie and R. K. Wakerling (McGraw-Hill, New York, 1949), Chap. 3.
[9] P. C. Stangeby, and G. M. McCracken, Nucl. Fusion **30**, 1225 (1990).
[10] R. Chodura, in *Physics of Plasma-Wall Interactions in Controlled Fusion* (Ref. [3]).
[11] L. D. Landau and E. M. Lifsits, *Fluid Mechanics* (Pergamon, London, 1959).
[12] C. M. Bender and S. O. Orszag, *Advanced Mathematical*

Methods for Scientists and Engineers (McGraw-Hill, New York, 1978).

[13] S. I. Braginskii, in *Reviews of Plasma Physics*, edited by M. A. Leontovich (Consultant Bureau, New York, 1965), Vol. 1.

[14] R. Cohen and D. D. Ryutov, Phys. Plasmas **2**, 2011 (1995).

[15] H. L. Berk, D. D. Ryutov, and Yu. A. Tsidulko, Phys. Fluids B **3**, 1364 (1991).

[16] J. Wesson, *Tokamaks*, 2nd ed. (Clarendon, Oxford, 1997).

[17] R. Simonini, G. Corrigan, G. Radford, J. Spence, and A. Taroni, Contrib. Plasma Phys. **34**, 368 (1994).